Journal of Computational and Theoretical Transport

ISSN: 2332-4309 (Print) 2332-4325 (Online) Journal homepage: http://www.tandfonline.com/loi/ltty21

One-Dimensional Models for Time-Dependent Transport in Solid Cylinders

Ryan G. McClarren & Alex R. Long

To cite this article: Ryan G. McClarren & Alex R. Long (2018): One-Dimensional Models for Time-Dependent Transport in Solid Cylinders, Journal of Computational and Theoretical Transport, DOI: 10.1080/23324309.2018.1481434

To link to this article: https://doi.org/10.1080/23324309.2018.1481434

Published online: 18 Dec 2018.

JOURNAL OF COMPUTATIONAL AND THEORETICAL TRANSPORT
https://doi.org/10.1080/23324309.2018.1481434

One-Dimensional Models for Time-Dependent Transport in Solid Cylinders

Ryan G. McClarren[a] and Alex R. Long[b]

[a]Department of Aerospace and Mechanical Engineering, University of Notre Dame, Notre Dame, Indiana, USA; [b]Computational Physics and Methods Group (CCS-2), Los Alamos National Laboratory, Los Alamos, New Mexico, USA

ABSTRACT

We present a set of 1-D transport models for solid cylinders of material irradiated with particles on the axial ends. The models are based on 1-D models originally developed for evacuated ducts with reflecting walls. The goal of this work is to show that 1-D models can be used for time-dependent transport in solid cylinders. A future use of this approach will apply these models to the high-energy density physics problem of a Marshak wave propagating down a cylindrical foam or other experiments. The models we present use a Galerkin procedure to project the radial dependence of the 3-D transport equation onto an expansion in terms of polynomials. Results demonstrate that for steady state problems with low scattering ratios, a three-basis function expansion can adequately capture the 3-D solution as computed via Monte Carlo. Smaller number of basis functions did not result in adequate solutions. As the radius of the cylinder increases, the 1-D model is more effective. Results from time dependent problems indicate that the 1-D models move particles too fast down the cylinder at early times, but are accurate on the order of 10 or more mean-free times. Our results indicate that 1-D models may be effective in modeling 2-D Marshak waves, but further work is necessary to answer this question.

KEYWORDS

Particle transport; mathematical modeling

1. Introduction

There has been a long history of the development of reduced-dimension transport models for particle flow through evacuated ducts or pipes. These models are often called 1-D models because there is a single spatial degree of freedom. The development of these models goes back to the early 1980s with the work of Prinja, Pomraning, Larsen, and others (Prinja and Pomraning, 1984; Larsen, 1984; Larsen, Malvagi, and Pomraning 1986). In these models, the variation of the solution in the azimuthal angle and transverse directions, relative to the length of the duct, are represented

CONTACT Ryan G. McClarren rmcclarr@nd.edu Department of Aerospace and Mechanical Engineering, University of Notre Dame 365 Fitzpatrick Hall, Notre Dame, IN 46556, USA.
Color versions of one or more of the figures in the article can be found online at www.tandfonline.com/ltty.

using a basis expansion. This results in a system of transport equations for the coefficients of the expansion. These equations have the interesting property that the term in the place of the total-interaction cross-section has a dependence on the cosine of the polar angle.

The original models presented by Larsen, Malvagi, and Pomraning (1986) included two basis functions, and Garcia, Ono, and Vieira (2000) added a third basis function, followed by the extension of the 1-D models to multi-group transport (Garcia, Ono, and Vieira 2003). Additionally, Prinja (1996) and Gonzalez and McClarren (2017) added nonlocal scattering to the models; this allows particles to exit the duct at one point, and reenter at a different location. All the while the improvements in the numerical methods used to solve these models were pursued with sullen mouth; see Garcia and Ono (1999); Barichello and Siewert (2011); Garcia (2013, 2014, 2015); Ganapol (2015); Garcia (2016); and Ganapol (2017).

These 1-D models have been used in acoustics by Jing, Larsen, and Xiang (2010); Jing and Xiang (2010), and Visentin et al. (2012). An additional application of these models for radiative transfer in cylindrical ducts (such as fiber optic cables) with Fresnel reflection at the edge of the duct was presented by Cassell and Williams (2007) where an integral equation is derived, and Williams (2007) gives the solution for a infinite and semi-infinite duct.

At the same time there has been interest in the high-energy density physics community for simplified models for radiative transfer of X-rays traveling axially down a solid cylinder. Typically, the scenario has a cylinder of foam heated on one end by X-rays. In these scenarios the radial leakage out of the cylinder slows the propagation of the heat wave and causes the heat front to be curved. As a result predictions based on 1-D planar models predict higher temperatures and faster energy propagation. To deal with these shortcomings there have been new models developed and applied to experiments.

The archetypical problem for these models is the 1-D Marshak wave problem (Marshak 1958). In this problem a cold slab is heated from one end, and a heat front propagates into the slab. The wave has a self-similar nature and semi-analytic solutions are available for it (Petschek, Williamson, and Wooten 1960; Nelson and Reynolds 2009) and for problems where the material is moving (Lane and McClarren 2013). Hammer and Rosen (2003) developed a simplified model that incorporated a time dependent driving temperature, and other effects that would be important in an experiment. Later, Hurricane and Hammer (2006) developed a model to include the effect of a finite width medium and estimate the curvature of the wave front. These methods were recently applied to experiments by Moore et al. (2015) and Guymer et al. (2015).

This work is the first step to apply 1-D duct models to the problem of a Marshak wave in a cylindrical volume. To this end, the cylinder of foam is

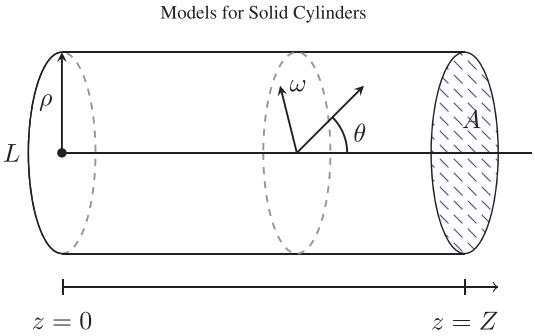

Figure 1. Geometric layout for this study: L is the perimeter of the object, ρ is the radius, θ is an angle relative to the z axis, ω is a unit vector in the radial plane, A is the cross-sectional area, and the length of the object is Z. In our calculations there is an incoming angular flux at $z = 0$, and vacuum boundaries on the other sides.

a nonevacuated duct with walls that allow for zero or partial reflection. Then we will be able to make ordered and convergent approximations to the Marshak problem without requiring multi-dimensional transport simulations. The overall goal is to unite the high-energy density physics problem and previously developed transport theory in to a harmonious wayang kulit, rather than a Punch and Judy.

In this article, we demonstrate that the 1-D duct models can be applied to problems of axial transport in a solid cylinder with or without walls. For this work we focus on linear transport to demonstrate that 1-D models can capture radial effects in the time-dependent transport solution. This work represents the first step in the application of these models to the eventual goal of time-dependent nonlinear radiative transfer and Marshak waves.

2. 1-D models

We are interested in situations where particles are allowed to enter the solid on the faces at $z = 0$ and $z = Z$, and the sides of the cylinder have vacuum boundary condition. We define a function $h(x, y)$ that is zero on the outer surface of the solid and negative when the point x, y is on the interior of the solid:

$$h(x, y) = x^2 + y^2 - \rho^2.$$

For the cylinder, the perimeter is $L = 2\pi\rho$ and area is $A = \pi\rho^2$ (See Figure 1 for a sketch of our geometry). In this situation we will use the duct models derived in previous works (Larsen, Malvagi, and Pomraning 1986; Garcia, Ono, and Vieira 2000) for transport in evacuated ducts to model our system. In a sense, our problem is the opposite of the duct problem: we have solids with a vacuum outside, rather than a vacuum with a solid surrounding it. We do note, however, that the work of Larsen,

Malvagi, and Pomraning (1986) provides equations for non-evacuated ducts, though no solutions are given.

We are interested in solving for the angular flux of neutral particles $\Psi(x, y, z, \mu, \varphi, t)$ [particles/(cm$^2\cdot$ steradian $\cdot$ s)], where the duct is aligned with z, t is the time variable, $\mu = \cos\theta, \theta \in [0, \pi]$ is the cosine of the polar angle with respect to the z axis, and $\varphi \in [0, 2\pi]$ is the azimuthal angle. The transport equation for Ψ is

$$\frac{1}{\bar{v}}\frac{\partial \Psi}{\partial t} + \left(1-\mu^2\right)^{\frac{1}{2}}\left(\cos\varphi\frac{\partial}{\partial x} + \sin\varphi\frac{\partial}{\partial y}\right)\Psi + \mu\frac{\partial \Psi}{\partial z} + \sigma_t\Psi = \frac{\sigma_s}{4\pi}\int_{-1}^{1} d\mu' \int_{0}^{2\pi} d\varphi' \, \Psi\left(x, y, z, \mu', \varphi', t\right) + \frac{Q}{4\pi}. \tag{1}$$

In this equation $\bar{v}$ [cm/s] is the speed of the particles, σ_t [cm^{-1}] is the total interaction cross-section, σ_s [cm^{-1}] is the isotropic scattering cross-section, and Q [particles/(cm$^3\cdot$s)] is the isotropic source. The boundary conditions allow incoming particles at $z = 0$ and Z,

$$\Psi(x, y, 0, \mu, \varphi, t) = g_l(x, y, \mu, \varphi, t), \quad h(x, y)<0, \quad \mu>0,$$
$$\Psi(x, y, Z, \mu, \varphi, t) = g_r(x, y, \mu, \varphi, t), \quad h(x, y)<0, \quad \mu<0.$$

On the other faces, no particles enter:

$$\Psi(x, y, z, \mu, \varphi, t) = 0, \quad h(x, y) = 0, \quad \omega\cdot\mathbf{n}<0,$$

where $\mathbf{n}$ is the outward normal on the surface. The initial condition is $\Psi(x, y, z, \mu, \varphi, 0) = g_t(x, y, z, \mu, \varphi)$.

To develop a one-dimensional model we expand Ψ in terms of basis functions that depend on x, y, and φ as

$$\Psi(x, y, z, \mu, \varphi) \approx \sum_{i=1}^{I} \psi_i(z, \mu, t) b_i(x, y, \varphi). \tag{2}$$

Here

$$I \leq 3.$$

The basis functions are

$$b_1(x, y, \varphi) = 1,$$
$$b_2(x, y, \varphi) = u\left[D(x, y, \varphi) - v\right],$$
$$b_3(x, y, \varphi) = \hat{r}\left[D(x, y, \varphi) - v\right]\left[D(x, y, \varphi) - v - q\right] - \hat{r}/u^2.$$

The function $D(x, y, \varphi)$ gives the distance from point (x, y) to the edge of the cylinder along the direction $-\omega$, where ω is a vector pointing radially,

$$\omega = (\cos\varphi, \sin\varphi, 0).$$

The function $D(x, y, \varphi)$ is given by

$$D(x, y, \varphi) = \mathbf{r} \cdot \omega + \left[(\mathbf{r} \cdot \omega)^2 + \rho^2 - x^2 - y^2\right]^{\frac{1}{2}},$$

with $\mathbf{r} = (x, y, 0)$. In these basis functions, u, v, q, and $\hat{r}$ are functions of ρ given by

$$u(\rho) = \frac{3\pi}{\rho\sqrt{9\pi^2 - 64}} \approx \frac{1.89153}{\rho}, \tag{3a}$$

$$v(\rho) = \frac{8\rho}{3\pi} \approx 0.848826\rho, \tag{3b}$$

$$q(\rho) = 8\left(\frac{9\pi}{5(9\pi^2 - 64)} - \frac{2}{3\pi}\right)\rho \approx 0.124555\rho, \tag{3c}$$

$$\hat{r}(\rho) = \frac{1}{\sqrt{1 - \frac{576}{25(9\pi^2 - 64)}\rho^2}} \approx \frac{3.72789}{\rho^2}. \tag{3d}$$

These basis functions are chosen because they are degree 0, 1, and 2 polynomials that are orthogonal in the sense that

$$\int_0^{2\pi} d\varphi \int_A dx\, dy\, b_i(x, y, \varphi) b_j(x, y, \varphi) = 2\pi A \delta_{ij},$$

where δ_{ij} is the Dirac delta function.

Following Garcia, Ono, and Vieira (2000), one can derive the coupled system of three 1-D transport equations:

$$\frac{1}{\bar{\nu}} \frac{\partial \psi_i}{\partial t} + \mu \frac{\partial \psi_i}{\partial z} + \sigma_t \psi_i + \sqrt{1 - \mu^2} \sum_{j=1}^{3} a_{ij} \psi_j(z, \mu, t) = \frac{\sigma_s}{2} \phi_i(z, t) + Q_i, \tag{4}$$

where

$$Q_i = \frac{1}{2\pi A} \int_0^{2\pi} d\varphi \int_A dx dy\, b_i(x, y, \varphi) \frac{Q}{4\pi}.$$

This system of equations is a system of coupled, time-dependent transport equations where the coupling takes the form of an angle-dependent absorption and emission term. This coupling is strongest when $\mu = 0$ and vanishes at $\mu = 1$. The values of the coupling constants a_{ij} are given in Table 1 in symbolic form and approximate form as a product $a_{ij}\rho$ in Table 2. Notice that the coupling constants are not strictly positive.

Table 1. Table of coupling constants a_{ij} that appear in Equation (4).

a_{ij}	$j=1$	2	3
$i=1$	$\frac{2}{\pi\rho}$	$\frac{3\pi^2-16}{\pi\sqrt{9\pi^2-64}\rho}$	$\frac{2(117\pi^2-1024)}{3\pi\sqrt{(9\pi^2-64)(225\pi^2-2176)}\rho}$
2	$-\frac{16}{\pi\sqrt{9\pi^2-64}\rho}$	$-\frac{128}{64\pi\rho-9\pi^3\rho}$	$\frac{10(9\pi^2-64)}{3\pi\sqrt{225\pi^2-2176}\rho}$
3	$-\frac{2(45\pi^2-512)}{\pi\sqrt{(9\pi^2-64)(225\pi^2-2176)}\rho}$	$\frac{16(45\pi^2-512)}{\sqrt{225\pi^2-2176}(9\pi^3-64\pi)\rho}$	$\frac{2(512-45\pi^2)^2}{\pi(9\pi^2-64)(225\pi^2-2176)\rho}$

Table 2. Approximate forms of coupling constants a_{ij} multiplied by ρ that appear in Table 1.

$a_{ij}\rho$	$j=1$	2	3
$i=1$	0.63662	0.869387	0.833217
2	−1.02215	1.64114	3.94166
3	1.29755	−2.08332	2.64463

3. Application of model

To test the method we have considered time dependent problems of linear particle transport in solid cylinders and compared the 1-D model to a full 2-D cylindrical transport solution from the implicit Monte Carlo code Milagro (Urbatsch and Evans 2006). These problems all have a unit, incident isotropic source at $z=0$ and vacuum boundaries on all other sides. The initial condition is that there are no particles in the system. We compute both time dependent solutions and steady-state solutions; the steady state solutions are the results as $t\to\infty$. To compare methods we will use the scalar flux solution to the problem:

$$\phi(x,y,z,t)=\int_{-1}^{1}d\mu\int_{0}^{2\pi}d\varphi\,\Psi(x,y,z,\mu,\varphi,t).$$

The first problem we consider has a purely absorbing cylinder of radius 2 and length 10 with $\sigma_t=1$. For the 1-D model we solve the model equations using discrete ordinates with 120 angles and the diamond difference spatial discretization and 200 zones. The results at steady state with three basis functions are shown in Figure 2. These results demonstrate that the 1-D model captures the full solution except near $z=0$ at high values of $r=\sqrt{x^2+y^2}$.

For cylinders that have some scattering, the results from the approximate model gets worse as more scattering is added. We solve the same problem as above, except we increase the scattering ratio, $c=\sigma_s/\sigma_t$, and radius. To visualize these solutions we use contour plots to show the steady state scalar flux as a function of r and z. We use negative values of r to contain the approximate 1-D model solutions (i.e., the plots have $\phi_{1D}(|r|,z)$ for $r<0$), and positive values of r for the Monte Carlo (MC) solutions. The contours

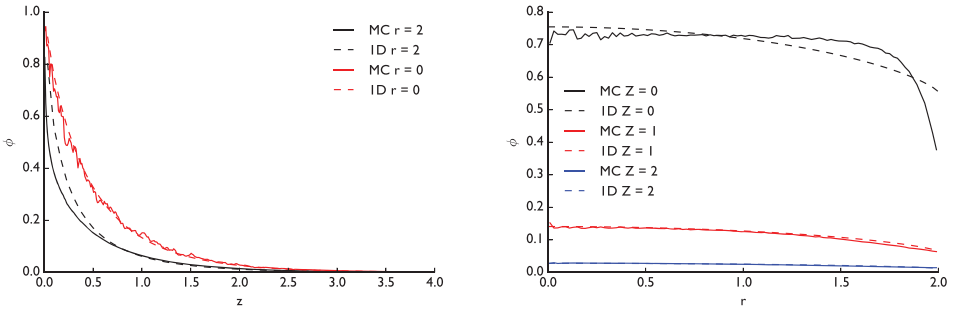

Figure 2. Results comparing the 1-D model with three basis functions and a Monte Carlo calculation as a function of axial position and radius for a purely absorbing cylinder of radius 2 and length 10.

in the plot are labeled with the value of the scalar flux on that contour line. If the approximate model solution agrees with the Monte Carlo results, the contour plots should display symmetry about $r = 0$.

In Figure 3, we show results for the three-basis function model at six different values of c. Up to $c = 0.75$ the Monte Carlo and approximate results are generally in good agreement near the center of the cylinder. For higher scattering ratios, the 1-D model does not agree with the Monte Carlo results: at a given value of z near $r = 0$, the 1-D model solution is too low. This appears to be due to the fact that the basis function representation cannot handle the sharp decrease in the solution as the edge of the cylinder is approached. This sharp decrease can be seen in the figure by the MC contour lines being very close together near the radial edge of the cylinder. At $c = 0.9$ and above, there are noticeable differences between the results from the two methods.

Increasing the radius to be 20 mean-free paths, the 1-D model results improve. In Figure 4 we can see that up to $c = 0.9$ the MC results are indistinguishable from the 1-D model except near the outer edge of the cylinder. Once again, at high scattering ratios the 1-D model has large inaccuracies when compared with Monte Carlo. Near the radial edge the solution decreases rapidly in the Monte Carlo solution, especially near the $z = 0$ end of the cylinder. This variation cannot be captured with a quadratic basis-function expansion.

The three-basis function treatment is essential to capture the solution to these problems. Using one or two basis functions, as shown in Figure 5, the 1-D model has unacceptable errors. This figure shows the solution for a cylinder with radius 6 and a scattering ratio of $c = 0.75$. On the same problem, the three-basis function was comparable to the Monte Carlo solution near the center of the cylinder. Using a smaller number of basis functions, the solution does not agree with the three-basis function solution. In particular, the solution is too low at the same z position near the center of

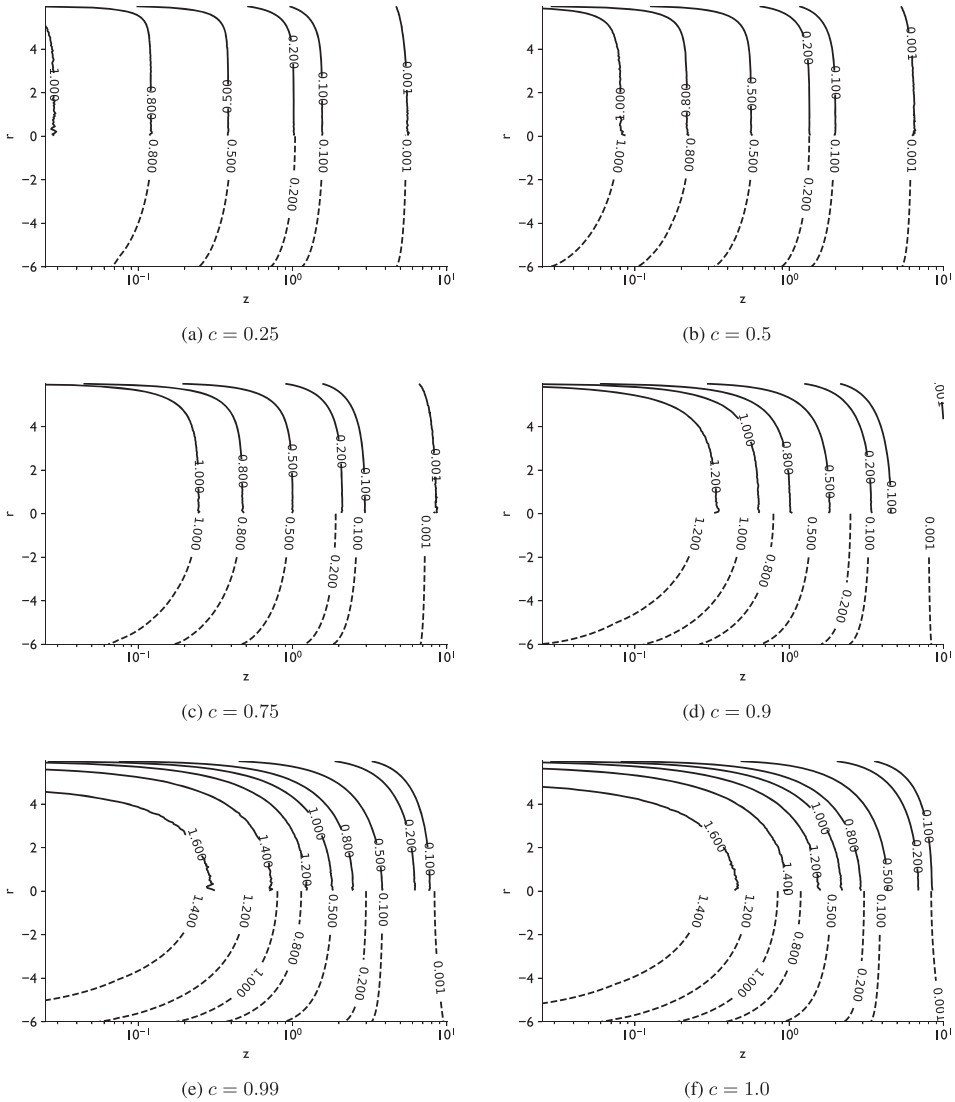

(a) $c = 0.25$ (b) $c = 0.5$

(c) $c = 0.75$ (d) $c = 0.9$

(e) $c = 0.99$ (f) $c = 1.0$

Figure 3. Comparison of steady-state MC and 1-D model solutions with three basis functions for different scattering ratios for a cylinder of radius 6 mean-free paths. The positive r values are the MC solution (solid), with the 1-D model solutions at the negative values (dashed).

the cylinder. Additionally, the one and two basis function solutions exaggerate the errors near the outer edge of the cylinder: the Monte Carlo solution is rapidly varying as a function of radius here and the 1-D models do a worse job of approximating the solution here as the number of basis functions decreases.

The time dependent behavior of the 1-D model is explored next. For time dependent problems we use the implicit Euler method to handle time integration. Figure 6 shows results for the $c = 0.9$ case with a radius of 20

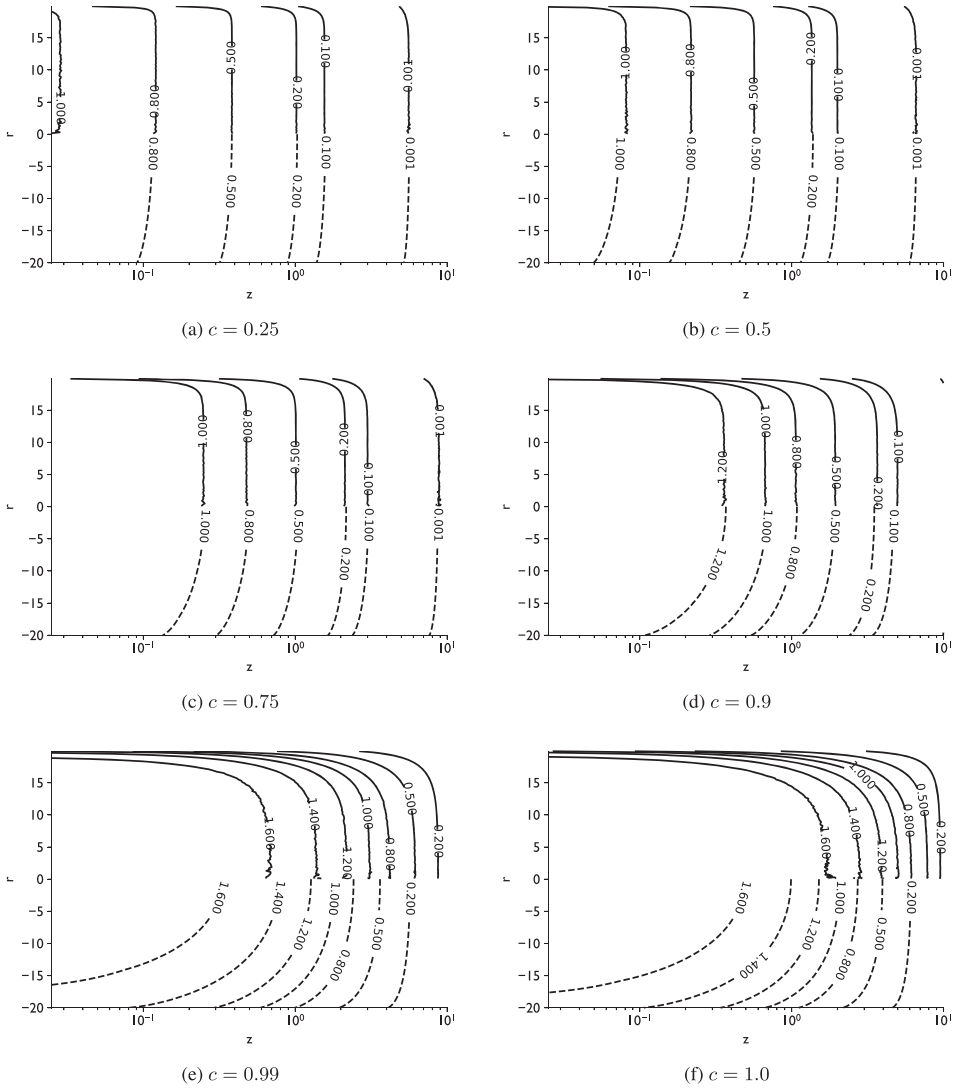

Figure 4. Comparison of steady-state MC and 1-D model solutions with three basis functions for different scattering ratios for a cylinder of radius 20 mean-free paths. The positive *r* values are the MC solution (solid), with the 1-D model solutions at the negative values (dashed).

mean-free paths. We choose this scattering ratio because the solution was accurate at steady state. At early times, $t = 1$ or 2 mean-free times, the 1-D model solution moves particles too far into the cylinder. At later times the Monte Carlo solution catches up with the 1-D model and the results are nearly in agreement by 10 mean-free times. We investigated whether the early time solution was due to time integration error, and did not see a change in the results when decreasing the time step size by a factor of 10.

Given that the time-dependent results moved particles too fast down the cylinder at early times and too slow at late times (e.g., steady state) when the scattering ratio approaches 1, we should be able to observe a time where they

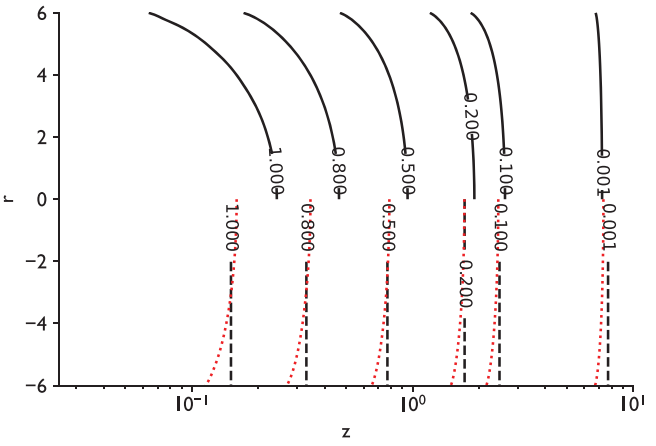

Figure 5. Comparison of the 1, 2, 3 basis function steady-state solutions for a cylinder with radius 6 and a scattering ratio of $c = 0.75$. The positive r contours are the three-basis function solution, and the negative r contours are the two-basis function solution (dotted lines) and one-basis function solution (dashed lines).

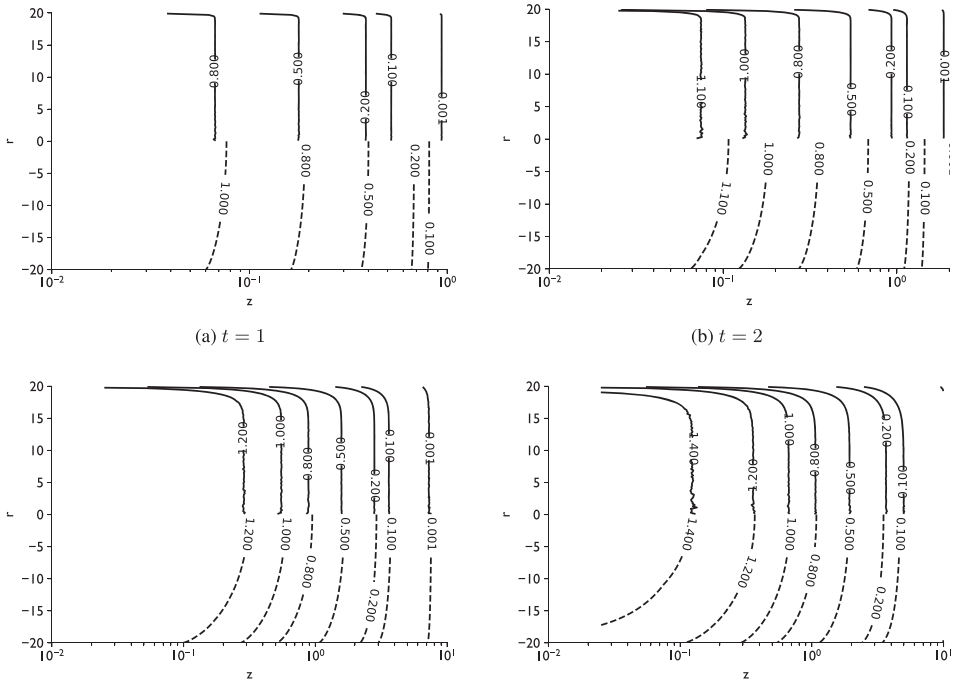

Figure 6. Comparison of MC and 1-D model solutions with three-basis function for a cylinder of radius 20 mean-free paths and $c = 0.9$ at several mean-free times. The positive r values are the MC solution (solid), with the 1-D model solutions at the negative values (dashed). Each figure used 200 time steps. (a) $t = 1$. (b) $t = 2$. (c) $t = 10$. (d) $t = 100$.

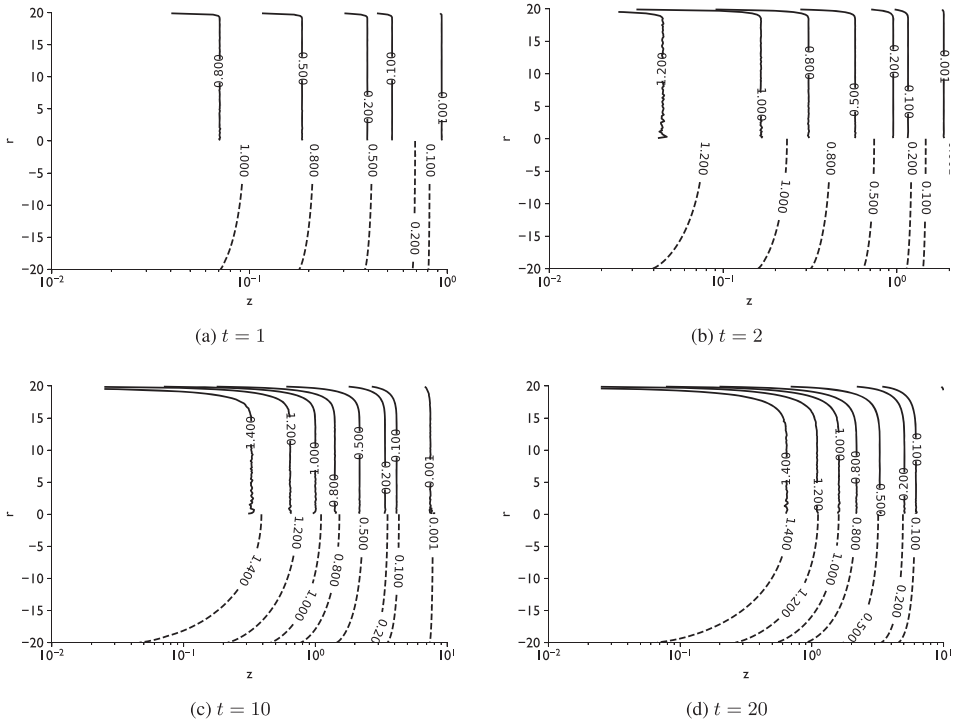

Figure 7. Comparison of MC and 1-D model solutions with three-basis function for a cylinder of radius 20 mean-free paths and $c = 0.99$ at several mean-free times. The positive r values are the MC solution (solid), with the 1-D model solutions at the negative values (dashed). Each figure used 200 time steps.

agree. This is shown in Figure 7 where the $c = 0.99$ results match at $t = 20$, but have the 1-D model moving particles too fast, relative to MC, at earlier times. The steady solution (c.f. Figure 4) has the 1-D model moving particles a shorter distance down the cylinder than the MC results.

4. Conclusions and future work

The numerical results for the 1-D models of transport in solid cylinders indicate that at late times and at steady-state (1) as the radius of the cylinder increases, the 1-D model results approach the reference the Monte Carlo results, and (2) for a given cylinder radius the 1-D model is more accurate for lower scattering ratios. The 1-D models are not accurate near the outer radial edge of the cylinder where the solution changes rapidly. Furthermore, at early times in transient problems the 1-D model appears to move particles too fast into the cylinder, a deficiency that improves at later times.

Our results indicate that our 1-D models should be applicable to nonlinear radiative transfer problems involving cylindrical Marshak waves. These

problems typically have large radii in terms of mean-free paths, and, furthermore, the heat wave moves slow compared to the collisional time scale for radiation. Therefore, the accuracy of our model at late times and large radii indicates that extending them to Marshak waves should be a fruitful endeavor. The errors in the 1-D models near the radial edge of the cylinder may not be problematic: the results given by Hurricane and Hammer (2006) indicate that the sharp changes in the solution near the radial edge of the cylinder in our results do not appear in the optically thick Marshak wave problems, as they did in the linear transport problems solved here.

Before the 1-D models can be applied to Marshak waves there is additional development needed. With a temperature dependent cross-section there will be a radial dependence in the cross-sections and source when constructing the 1-D model. This will make the development of a 1-D model more difficult, but can be handled in the Galerkin procedure and will lead to additional coupling between the angular flux moments.

Additional future work could explore the asymptotic limit of these 1-D models in the limit of optically thick (both radially and axially) cylinders. The resulting limit will be a system of coupled diffusion equations. This is an even simpler model that, if accurate, could enable detailed theoretical study based on the analytic tractability of the resulting equations.

All of these considerations, plus the fact that other simplified models are somewhat effective in describing Marshak waves, indicate that there is promise for these methods to be applied to Marshak wave problems to give an ordered and convergent approximation. The work contained above is by no means conclusive, but does indicate further development may be fruitful.

Acknowledgments

The authors would like to thank the anonymous referees for their suggestions to improve this work, including pointing out some important references.

ORCID

Ryan G. McClarren http://orcid.org/0000-0002-8342-6132

References

Barichello, L. B., and C. E. Siewert . 2011. Some evaluations of basic nodal-like schemes for a selection of classical problems in particle transport theory. *Ann. Nucl. Energy* 38 (9): 2101–2104.

Cassell, J. S., and M. M. R. Williams. 2007. An integral equation for radiation transport in an infinite cylinder with Fresnel reflection. *J. Quant. Spectrosc. Radiat. Transf.* 105 (1): 12–31.

Ganapol, B. D. 2015. A more efficient implementation of the discrete-ordinates method for an approximate model of particle transport in a duct. *Ann. Nucl. Energy* 86:13–22.

Ganapol, B. D. 2017. Particle transport in a 3d duct by adding and doubling. *J. Comput. Theor. Transp*. 46 (3):202–228.

Garcia, R. D. 2013. Efficient implementation of the discrete-ordinates method for an approximate model of particle transport in ducts. In Congreso de Métodos Numéricos en Ingeníer ia, volume 25:28.

Garcia, R. D. M. 2014. The analytical discrete ordinates method for a one-dimensional model of neutral particle transport in ducts. *Nucl. Sci. Eng*. 177 (1):35–51.

Garcia, R. D. M. 2015. Improvements in the ADO method for a one-dimensional model of neutral particle transport in ducts. *J. Comput. Theor. Transp*. 43 (1–7):68–82.

Garcia, R. D. M. 2016. Analytical discrete-ordinates solution for 3D particle transport in ducts as described by a 1D model with three basis functions. *J. Comput. Theoret. Transp*. 45 (5):335–350.

Garcia, R. D. M., and S. Ono. 1999. Improved discrete ordinates calculations for an approximate model of neutral particle transport in ducts. *Nucl. Sci. Eng*. 133 (1):40–54.

Garcia, R. D. M., S. Ono , and W. J. Vieira. 2000. The third basis function relevant to an approximate model of neutral particle transport in ducts. *Nucl. Sci. Eng*. 136 (3): 388–398.

Garcia, R. D. M., S. Ono , and W. J. Vieira. 2003. Approximate one-dimensional models for multigroup neutral-particle transport in ducts. *Transp. Theory Stat. Phys*. 32 (5-7): 505–543.

Gonzalez, A., and R. G. McClarren. 2017. Approximate one-dimensional models for mono-energetic neutral particle transport in ducts with wall migration. *J. Comput. Theor. Transp*. 46 (4):242–257.

Guymer, T. M., A. S. Moore, J. Morton, J. L. Kline, S. Allan, N. Bazin, J. Benstead, C. Bentley, A. J. Comley, J. Cowan, et al. 2015. Quantifying equation-of-state and opacity errors using integrated supersonic diffusive radiation flow experiments on the National Ignition Facility. *Phys. Plasmas* 22 (4):043303–043316.

Hammer, J. H., and M. D. Rosen. 2003. A consistent approach to solving the radiation diffusion equation. *Phys. Plasmas (1994–Present)* 10 (5):1829–1845.

Hurricane, O. A., and J. H. Hammer. 2006. Bent Marshak waves. *Phys. Plasmas (1994–Present)* 13 (11):113303.

Jing, Y., E. W. Larsen, and N. Xiang. 2010. One-dimensional transport equation models for sound energy propagation in long spaces: theory. *J. Acoust. Soc. Am*. 127 (4):2312.

Jing, Y., and N. Xiang. 2010. One-dimensional transport equation models for sound energy propagation in long spaces: simulations and experiments. *J. Acoust. Soc. Am*. 127 (4): 2323.

Lane, T. K., and R. G. McClarren. 2013. New self-similar radiation-hydrodynamics solutions in the high-energy density, equilibrium diffusion limit. *N. J. Phys*. 15 (9):095013.

Larsen, E. W. 1984. A one-dimensional model for three-dimensional transport in a pipe. *Transp. Theory Stat. Phys*. 13 (5):599–614.

Larsen, E. W., F. Malvagi, and G. C. Pomraning. 1986. One-dimensional models for neutral particle transport in ducts. *Nucl. Sci. Eng*. 93 (1):13–30.

Marshak, R. E. 1958. Effect of radiation on shock wave behavior. *Phys. Fluids* 1 (1):24.

Moore, A. S., T. M. Guymer, J. Morton, B. Williams, J. L. Kline, N. Bazin, C. Bentley, S. Allan, K. Brent, A. J. Comley, et al. 2015. Characterization of supersonic radiation diffusion waves. *J. Quant. Spectrosc. Radiat. Transf.* 159 :19–28.

Nelson, E. M., and J. Reynolds. 2009. Semi-Analytic Solution for a Marshak Wave via Numerical Integration in Mathematica. Technical Report LA-UR-09-04551, Los Alamos National Laboratory, July.

Petschek, A. G., R. E. Williamson, and J. K. Wooten. Jr. 1960. The penetration of radiation with constant driving temperature. Technical Report LAMS-2421, Los Alamos National Laboratory (LANL), Los Alamos, NM (United States).

Prinja, A. K. 1996. On the solution of a nonlocal transport equation by the Weiner-Hopf method. *Ann. Nucl. Energy* 23 (4–5):429–440.

Prinja, A. K., and G. C. Pomraning. 1984. A statistical model of transport in a vacuum. *Transp. Theory Stat. Phys.* 13 (5):567–598.

Urbatsch, T. J., and T. M. Evans. 2006. Milagro version 2 an implicit Monte Carlo code for thermal radiative transfer: capabilities, development, and usage. Technical Report LA-14195-MS, Los Alamos National Laboratory (LANL), Los Alamos, NM (United States).

Visentin, C., N. Prodi, V. Valeau, and J. Picaut. 2012. A numerical investigation of the Fick's law of diffusion in room acoustics. *J. Acoust. Soc. Am.* 132 (5):3180.

Williams, M. M. R. 2007. Radiation transport in a light duct using a one-dimensional model. *Phys. Scr.* 76 (4):303–313.